Vapor-Liquid Equilibrium in the System Carbon Dioxide + 2,2-Dimethylpropane from 262 to 424 K at Pressures to 8.4 MPa

Nilesh N. Shah,[†] Maria E. Pozo de Fernández,[‡] John A. Zollweg,* and William B. Streett

School of Chemical Engineering, Olin Hall, Cornell University, Ithaca, New York 14853

Isothermal vapor-liquid equilibrium data have been measured for the carbon dioxide/2,2-dimethylpropane system at 11 temperatures from 261.93 to 423.55 K and at pressures to 8.31 MPa. The mixture critical line has been located and is shown to be continuous in $p-T-x$ space between the critical points of the pure components. The results are compared with other measurements. The data sets are also correlated by using two cubic equations of state, the Soave-Redlich-Kwong and Peng-Robinson equations. Binary interaction parameters for the system are reported for both equations of state over the entire temperature range.

Introduction

This study is a continuation of a research program to provide vapor-liquid equilibrium (VLE) data over a wide range of temperatures on binary systems of interest to the petroleum and natural gas industry. VLE data for CO_2/pentane (*1*) and CO_2/butane (*2*) have been reported previously, and VLE data for CO_2/cyclopentane are being reported in a companion paper (*3*).

The binary system CO_2/2,2-dimethylpropane (neopentane) has been studied by Schwartz and Donnelly (*4*), Stead and Williams (*5*), and Leu and Robinson (*6*). This paper presents VLE data for this system at temperatures from 262 to 424 K and at pressures to the critical line of the mixture.

Experimental Section

The apparatus and the procedure used in this study are essentially the same as those used by Pozo and Streett (*7*) and Chang, Calado, and Streett (*8*) in their studies of dimethyl ether/water and dimethyl ether/methanol, respectively. It is a vapor recirculation system designed for the measurement of liquid- and vapor-phase compositions as a function of pressure at fixed temperature. The details of the method have been given in earlier papers (*7*, *8*) and by Tsang and Streett (*9*).

Two apparatuses were used in this study, depending on the temperature. The high-temperature apparatus (working temperature range 325-530 K) is a modification of the one used by Pozo and Streett (*7*). A schematic diagram of it is shown in Figure 1. The principal difference from the earlier apparatus is that the equilibrium cell A is made from a commercial sight gage with a glass window. This cell is connected by a closed loop of tubing to the magnetically operated pump C. The pump withdraws vapor from the top of the cell and bubbles it through the liquid, the direction of flow being indicated by arrows in the figure. This bubbling action provides intimate contact between the phases and establishes equilibrium in 5-10 min. The volume of the cell was reduced by placing some stainless steel rods in it.

Temperature control within ±0.02 K up to 530 K was provided by a commercial windowed oven H. The glass window provides visibility of the fluid and is very useful for observing the onset of critical phenomena in the mixture. Temperatures were measured with a platinum resistance thermometer F and Mueller bridge and are accurate to ±0.002 K. Pressures are measured with an uncertainty of 0.07 MPa or 0.5% (whichever is greater) by a digital pressure gauge (Autoclave Eingineers, Inc., Model DPS-0021) calibrated in this laboratory against a Ruska DDR-6000 direct-reading quartz spiral gauge.

Vapor and liquid samples are withdrawn from the cell for analysis of their compositions through a sampling system. To overcome possible errors in composition due to partial condensation during throttling, a sampling cell D is placed in an insulated and separately heated chamber J inside the oven H (see Figure 1). The chamber J is heated to a temperature of 373 K or 20 K above the oven temperature, whichever is higher. The liquid sample is withdrawn into the previously evacuated sampling cell D, where it is allowed to stand for sufficient time to vaporize and become well mixed (about 10 min) before being transferred into the sampling loop of the gas chromatograph. The sampling cell is fitted with a 30 psig pressure relief valve R, with an outlet inserted into a small beaker of oil E, to serve as an overflow and to indicate when the sampling cell is filled. The heated sampling valves are fitted with long stems that pass through the oven wall to permit operation from outside the oven. The line between the sample cell and the gas chromatograph is heated to 373 K.

For the isotherms below 325 K, a modification of the apparatus of Chang, Calado, and Streett (*8*) was used. This apparatus is similar to the high-temperature apparatus described above except that it employs a liquid bath for temperature control instead of an air bath. A mixture of water and commercial antifreeze (after removing the dye by distillation) was used as bath fluid. The temperature of the bath was controlled within ±0.02 K by a Braun Model 1480 BKU proportional controller. To reach temperatures down to 273 K, a separately refrigerated coolant, also a mixture of ethylene glycol and water, was circulated through a coil in the controller. Below 273 K, this arrangement was not able to remove heat at a sufficient rate; hence liquid nitrogen was circulated through a separate coil immersed directly in the bath.

As with the high-temperature apparatus, the principal modification that was made to the previous apparatus was to replace the equilibrium cell. In this case, an equilibrium cell made from a sapphire tube was used as shown in Figure 2. The sapphire tube was confined between stainless steel flanges. Stainless steel mushrooms, sleeves, and Teflon gaskets provided a seal according to the Bridgman unsupported-area principle. The sleeves fit into grooves in the flanges, and 0.156-cm-o.d. stainless steel tubes were soldered to the mushrooms to provide access to the cell. The cell was also connected to the pump through these tubes as in the high-temperature apparatus. The rest of the assembly is the same as that of the high-temperature apparatus.

Gas samples were analyzed with a programmable gas chromatograph (Hewlett-Packard Model 5840A), with a thermal conductivity detector, a built-in digital process control, and an automatic sampling valve. A stainless steel column, 0.312-cm o.d., 50.8-cm length, packed with 100/120 mesh Porapak-Q, was used for separation of CO_2 and 2,2-dimethylpropane.

[†] Present address: Department of Chemical Engineering, University of California at Berkeley, Berkeley, California 94720.
[‡] Present address: Dpto. de Termodinámica y Fenómenos de Transferencia Universidad Simón Bolivar, Caracas 1086-A, Venezuela.

0021-9568/90/1735-0278$02.50/0

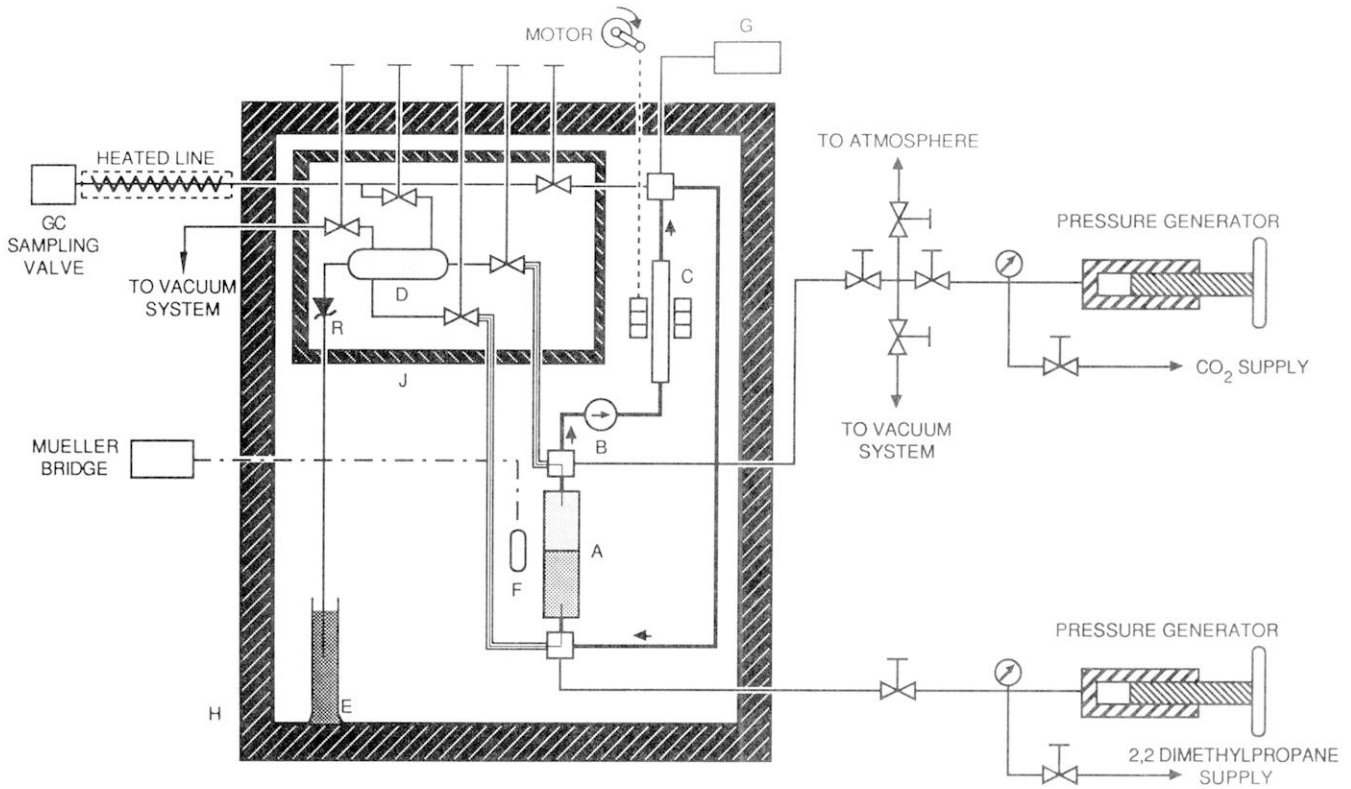

Figure 1. Schematic diagram of high-temperature vapor–liquid equilibrium apparatus. Components are labeled as follows: A, equilibrium cell; B, check valve; C, magnetically actuated recirculation pump; D, sampling chamber; E, beaker of oil; F, platinum resistance thermometer; G, digital pressure gauge; H, oven; J, heated chamber. The heavy line from the equilibrium cell through the check valve and the magnetic pump indicates the recirculation loop.

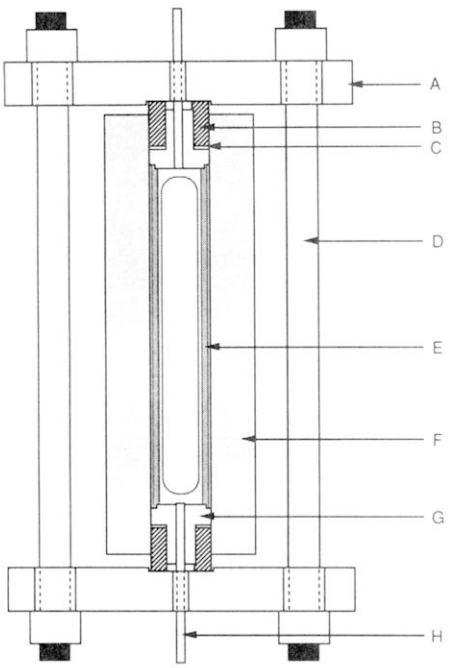

Figure 2. Detail of sapphire-tube pressure vessel. Components are labeled as follows: A, flange; B, sleeve; C, Teflon gasket; D, threaded rod; E, spacer; F, sapphire tube; G, mushroom plug; H, stainless steel tube.

Helium gas was used as a carrier at 25 cm^3/min. The column temperature was initially set at 353 K, with a 28 K/min temperature rise following emergence of the CO_2 peak (about 0.5 min after the start of the run), to accelerate the emergence of the 2,2-dimethylpropane peak. The gas chromatograph was calibrated with mixtures of known composition that were prepared gravimetrically. The phase compositions reported here are estimated to be accurate within ±0.2 mol % near the middle of the mole fraction range and better near the extremes. In the immediate vicinity of the critical line, the uncertainty may be as large as 0.5%.

The CO_2 used in this work was supplied by Air Products and Chemicals Inc., and had a purity of 99.99 mol %. The 2,2-dimethylpropane was supplied by Phillips Petroleum Co. with a purity of 99.99 mol %. These chemicals were used without further purification.

Results

Vapor and liquid compositions have been measured at 11 temperatures from 261.93 to 423.55 K and pressures to 8.3 MPa. The experimental results are recorded in Table I, and the isotherms are plotted on a pressure–composition ($p-x$) diagram in Figure 3. The system exhibits very small positive deviations from Raoult's law at low pressures. The pressure–temperature ($p-T$) extent of the region covered by this study is shown in Figure 4. AB and CD are the vapor pressure curves for CO_2 and 2,2-dimethylpropane, respectively, with critical points B and D. BED is the mixture critical line. Data for the pure components and mixture critical points are listed in Table II. In the critical region, phase compositions were measured at pressures within ~0.1 MPa of the critical pressure. The critical point of each isotherm was located by performing an extrapolation using the phase equilibrium values at the four or five highest pressures in an algorithm which is based on the assumption that the variation of composition with pressure about the critical value is cubic. In Figure 5, K values are plotted as a function of pressure ($K_i \equiv y_i/x_i$, where y_i is the mole fraction of component i in the vapor phase and x_i the corresponding mole fraction in the liquid phase) for four representative isotherms. Below the critical temperature of CO_2, an isotherm in the K-value diagram is composed of two separate branches, one for each component, with K values for CO_2, the more volatile component, al-

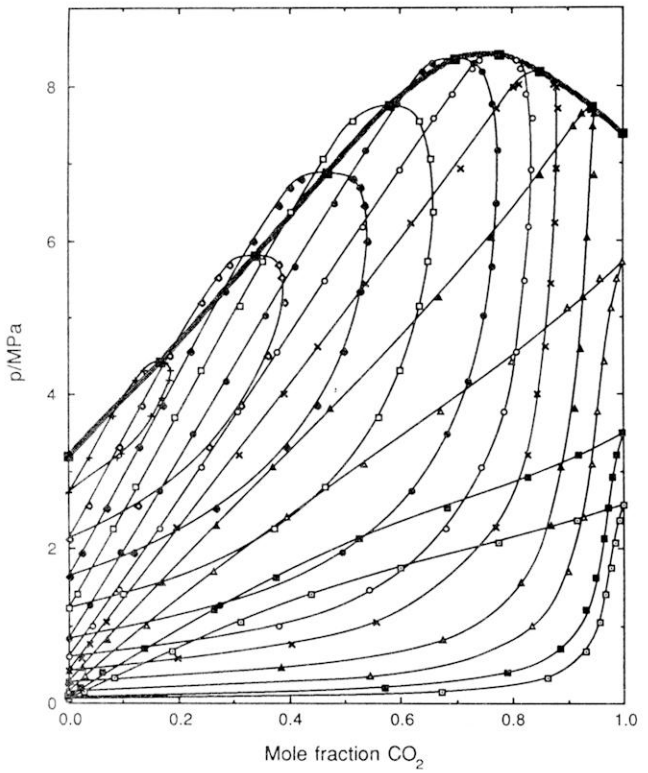

Figure 3. Experimental isotherms for the carbon dioxide/neopentane system. Symbols denote isotherms as follows: ⊡, 261.93 K; ■, 273.11 K; △, 292.99 K; ▲, 313.02 K; ×, 329.70 K; O, 343.31 K; ●, 358.35 K; □, 377.98 K; ♦, 393.50 K; ◇, 408.39 K; +, 423.55 K. Critical points are denoted by ■, and the critical line is shown as a wide shaded curve.

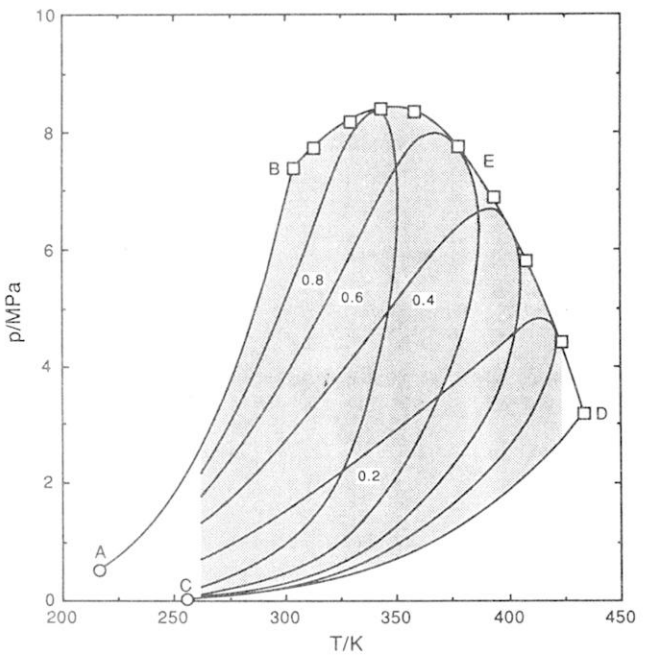

Figure 4. Pressure–temperature diagram for carbon dioxide/neopentane. The shaded area is the $p-T$ region covered in this work. AB and CD are the vapor pressure curves of carbon dioxide and neopentane, respectively, and BED is the mixture critical line. Critical points are denoted by □ and triple points by O. Four isopleths are also shown. Each is labeled with its mole fraction of CO_2 below the liquid branch.

ways greater than unity and the K values for 2,2-dimethylpropane less than unity. At temperatures between the critical values for the two pure components, the two branches converge at a critical point, where $K = 1$, and the curve has a vertical tangent at that point. Smooth K-value plots indicate consistency of the VLE data, as they tend to exaggerate scatter in the results.

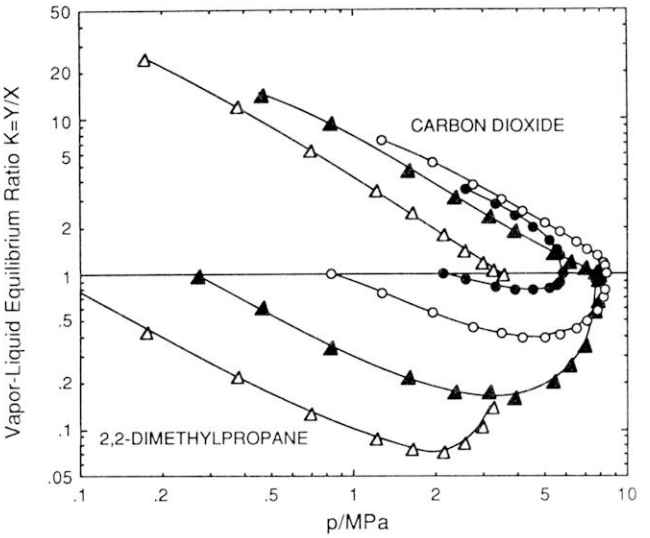

Figure 5. Equilibrium ratios for carbon dioxide/neopentane at four temperatures. The symbols denote isotherms as follows: △, 273.11 K; ▲, 313.02 K; O, 358.35 K; ●, 408.39 K.

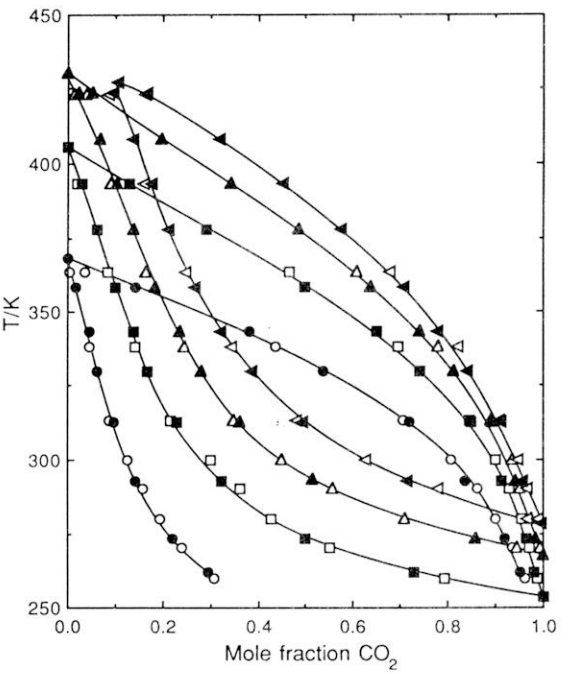

Figure 6. Temperature–mole fraction diagram for carbon dioxide/2,2-dimethylpropane. The symbols denote isobars as follows: circles, 1 MPa; squares, 2 MPa; triangles pointing up, 3 MPa; triangles pointing left, 4 MPa. The filled symbols were interpolated from isotherms reported in this work, the open symbols from the literature. Data for temperatures up to and including 300 K were from Stead and Williams and, for higher temperatures, from Leu and Robinson.

Comparison with Published Data

A literature search showed three previous studies of this system. Schwartz and Donnelly (*4*) studied solid + liquid + vapor equilibrium up to 257 K, while Stead and Williams (*5*) studied VLE up to 300 K. Leu and Robinson (*6*) measured five isotherms from 313 to 423 K. A comparison of Stead and Williams' and Leu and Robinson's data with our measurements is shown in Figure 6. The data have been cross-plotted on a $T-x$ diagram at four different pressures. This figure shows that the two sets of data match reasonably, but the Leu–Robinson

Table I. Equilibrium Phase Properties of the Carbon Dioxide (1)/2,2-Dimethylpropane (2) System

p, MPa	x_1	y_1	p, MPa	x_1	y_1	p, MPa	x_1	y_1
				T = 261.43 K				
0.0464	0.000	0.000	1.048	0.312	0.956	2.082	0.773	0.984
0.138	0.028	0.672	1.400	0.439	0.968	2.365	0.915	0.992
0.317	0.083	0.864	1.758	0.600	0.977	2.562	1.000	1.000
0.669	0.188	0.932						
				T = 273.11 K				
0.0724	0.000	0.000	1.186	0.266	0.935	2.910	0.829	0.982
0.172	0.023	0.574	1.606	0.378	0.953	3.192	0.922	0.989
0.372	0.064	0.793	2.106	0.529	0.966	3.4804	1.000	1.000
0.683	0.139	0.889	2.510	0.685	0.974			
				T = 292.99 K				
0.145	0.000	0.000	2.392	0.397	0.928	5.112	0.902	0.979
0.338	0.031	0.545	3.089	0.535	0.944	5.481	0.959	0.990
1.000	0.143	0.835	3.765	0.673	0.955	5.7067	1.000	1.000
1.689	0.264	0.900	4.420	0.800	0.966			
				T = 313.02 K				
0.265	0.000	0.000	3.054	0.371	0.888	6.836	0.852	0.948
0.455	0.026	0.385	3.813	0.475	0.913	7.470	0.910	0.947
0.807	0.070	0.675	4.585		0.923	7.639	0.927	0.950
1.558	0.170	0.814	5.261	0.669	0.930	7.701	0.941	0.945
2.296	0.270	0.870	6.033	0.764	0.937			
				T = 329.70 K				
0.4222	0.000	0.000	3.220	0.309	0.827	6.924	0.709	0.880
0.579	0.023	0.198	3.999	0.392	0.845	7.707	0.772	0.882
0.752	0.037	0.404	4.626	0.452	0.861	7.978	0.802	0.880
1.048	0.068	0.557	5.433	0.538	0.870	8.023	0.811	0.876
2.268	0.196	0.768	6.233	0.620	0.878			
				T = 343.31 K				
0.5887	0.000	0.000	3.771	0.307	0.785	7.577	0.660	0.837
1.000	0.044	0.381	4.551	0.377	0.807	7.888	0.692	0.825
1.455	0.091	0.543	5.474	0.464	0.822	8.212	0.728	0.814
2.261	0.164	0.680	6.171	0.532	0.831	8.315	0.742	0.808
3.047	0.241	0.743	6.909	0.600	0.836			
				T = 358.35 K				
0.8242	0.000	0.000	4.164	0.286	0.721	7.164	0.539	0.774
1.269	0.038	0.274	5.012	0.358	0.749	7.770	0.593	0.765
1.944	0.095	0.495	5.654	0.411	0.763	8.177	0.639	0.747
2.744	0.164	0.620	6.488	0.481	0.772	8.287	0.658	0.732
3.482	0.227	0.683						
				T = 377.98 K				
1.2277	0.000	0.000	3.696	0.194	0.560	6.378	0.403	0.659
1.413	0.014	0.099	4.316	0.242	0.599	7.053	0.462	0.655
2.248	0.081	0.372	5.150	0.312	0.634	7.550	0.515	0.634
2.792	0.123	0.465	5.730	0.353	0.650			
				T = 393.50 K				
1.6384	0.000	0.000	3.871	0.170	0.448	6.467	0.380	0.535
1.944	0.024	0.116	4.564	0.222	0.497	6.688	0.402	0.527
2.523	0.068	0.267	5.343	0.284	0.528	6.805	0.422	0.515
3.327	0.128	0.393	5.985	0.335	0.541			
				T = 408.39 K				
2.1218	0.000	0.000	3.868	0.133	0.313	5.516	0.272	0.386
2.558	0.035	0.124	4.513	0.182	0.360	5.681	0.291	0.380
3.323	0.091	0.254	5.199	0.240	0.390			
				T = 423.55 K				
2.7216	0.000	0.000	3.716	0.082	0.150	4.192	0.123	0.183
3.185	0.037	0.088	3.951	0.099	0.169	4.323	0.138	0.186
3.227		0.097						

Table II. Critical Line of Carbon Dioxide + 2,2-Dimethylpropane

T, K	p, MPa	amt of CO_2 ($x_1 = y_1$)	T, K	p, MPa	amt of CO_2 ($x_1 = y_1$)
304.19	7.382	1.000	377.98	7.743	0.581
313.02	7.729	0.944	393.50	6.878	0.470
329.70	8.169	0.850	408.39	5.792	0.341
343.31	8.390	0.778	423.55	4.420	0.168
358.35	8.342	0.697	433.75	3.196	0.000

data are significantly smaller than ours at small mole fractions of CO_2.

Equation of State Calculations

The experimental data have been compared with the predictions of two equations of state, the Soave–Redlich–Kwong (SRK) equation (*10*) and the Peng–Robinson (PR) equation (*11*):

SRK equation
$$p = \frac{RT}{V - b} - \frac{a(T)}{V(V + b)} \quad (1)$$

PR equation
$$p = \frac{RT}{V - b} - \frac{a(T)}{V(V + b) + b(V - b)} \quad (2)$$

Table III. Results of Data Analysis Using the SRK and PR Equations of State for the System Carbon Dioxide/2,2-Dimethylpropane

T, K	EOS	k_{12}	rms(x)	rms(y)
261.93	PR	0.088	0.0059	0.0034
	SRK	0.093	0.0067	0.0026
273.11	PR	0.094	0.0079	0.0043
	SRK	0.099	0.0102	0.0063
292.99	PR	0.097	0.0092	0.0059
	SRK	0.104	0.0082	0.0066
313.02	PR	0.093	0.0142	0.0120
	SRK	0.103	0.0144	0.0109
329.70	PR	0.108	0.0158	0.0274
	SRK	0.123	0.0187	0.0204
343.31	PR	0.124	0.0154	0.0287
	SRK	0.136	0.0183	0.0189
358.35	PR	0.136	0.0167	0.0311
	SRK	0.166	0.0151	0.0252
377.98	PR	0.158	0.0116	0.0229
	SRK	0.168	0.0076	0.0118
393.50	PR	0.171	0.0080	0.0244
	SRK	0.182	0.0048	0.0134
408.59	PR	0.188	0.0048	0.0228
	SRK	0.203	0.0033	0.0156
423.40	PR	0.222	0.0021	0.0149
	SRK	0.250	0.0016	0.0108

The parameters a and b are concentration dependent. The mixing rules for binary mixtures are

SRK

$$a = a_{11}x_1^2 + 2a_{12}x_1x_2 + a_{22}x_2^2 \quad (3)$$

$$b = b_{11}x_1^2 + 2b_{12}x_1x_2 + b_{22}x_2^2 \quad (4)$$

PR

$$a = a_{11}x_1^2 + 2a_{12}x_1x_2 + a_{22}x_2^2 \quad (5)$$

$$b = b_{11}x_1 + b_{22}x_2 \quad (6)$$

where

$$a_{12} = (1 - k_{12})(a_{11}a_{22})^{1/2} \quad (7)$$

$$b_{12} = (1 - j_{12})(b_{11} + b_{22})/2 \quad (8)$$

For both equations, the temperature dependence of the constant a is given by an expression based on the Pitzer acentric factor (*10*, *11*). The parameters b_{11} and b_{22} are evaluated from critical data for the pure components.

The binary interaction parameter k_{12} is calculated for each isotherm individually to compare the best fit by the equations of state with the experimental data. No attempt was made to optimize the fit by adjusting the binary parameter j_{12}, which was taken to be zero for this work. The values of k_{12} so calculated are presented in Table III along with the root mean square deviations of the vapor, rms(y), and liquid, rms(x), compositions. Three typical isotherms are plotted in Figure 7. The fit of both equations of state to the data are comparable. Both equations give better fits for the isotherms below the critical temperature of CO_2. At higher temperatures, the fit for the SRK equation is marginally better than for the PR equation. One can see in Figure 7 that, for the isotherm that is slightly above the critical temperature of CO_2, the cubic equations give a critical pressure that is smaller than the experimental value. This seems to be related to the fact that the experimental curve has a narrow and somewhat pointed top, which the cubic equation is unable to reproduce. The isotherm at the next lower temperature (shown in Figure 3) exhibits this behavior even more strongly. Both equations predict vapor-phase-composition values lower than the experimental values, especially at the higher temperatures. Adjustment of k_{12} allows one to obtain good agreement either with liquid compositions or with the critical pressure, but not with both (see Figure 7). The predicted vapor compositions are relatively insensitive to k_{12}.

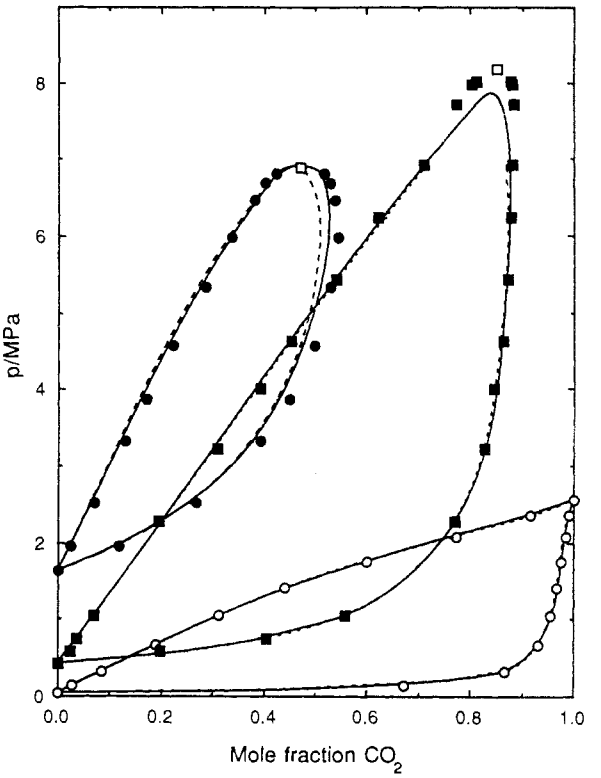

Figure 7. Comparison of three isotherms with equation of state calculations. Symbols denote isotherms as follows: ○, 261.93 K; ■, 329.70 K; ●, 393.50 K. The predictions of the Soave–Redlich–Kwong equation are shown by solid lines and the Peng–Robinson equation by dashed lines.

By adjusting j_{12}, the fit of the SRK equation to the data could have been improved, but it would no longer be possible to compare the SRK and PR equations on equal footing, because one would have two adjustable parameters and the other would have one adjustable parameter. The fact that substantially different values of k_{12} are required for adequate fits to the low- and high-temperature data indicates a fundamental deficiency in applying such cubic equations with only one adjustable parameter to systems of this sort. It is probable that nonquadratic mixing rules of the kind proposed by Panagiotopoulos and Reid (*12*) would give better results. At the level of two adjustable parameters, it would be interesting to compare the nonquadratic mixing rules with the SRK and PR equations and also to see whether adjusting j_{12} while keeping the quadratic mixing rule would give satisfactory results.

List of Symbols

a,b	coefficients in cubic equation of state
a_{ij},b_{ij}	coefficients in quadratic mixing rules for equation of state
j_{ij}	interaction parameter describing deviations from the linear combining rule for covolumes in the SRK equation
k_{ij}	interaction parameter describing deviations from the geometric mean combining rule for the unlike pair attraction parameter in cubic equations
K_i	$\equiv y_i/x_i$
p	absolute pressure
R	gas constant
rms(x,y)	root mean square deviation between calculated and experimental mole fractions on one isotherm
T	absolute temperature
V	molar volume
x_i	liquid mole fraction of component i

y_i vapor mole fraction of component i

Registry No. CO_2, 124-38-9; 2,2-dimethylpropane, 463-82-1.

Literature Cited

(1) Cheng, H.; Pozo de Fernández, M. E.; Zollweg, J. A.; Streett, W. B. *J. Chem. Eng. Data* **1989**, *34*, 319.
(2) Pozo de Fernández, M. E.; Zollweg, J. A.; Streett, W. B. *J. Chem. Eng. Data* **1989**, *34*, 324.
(3) Shah, N. N.; Zollweg, J. A.; Streett, W. B. *J. Chem. Eng. Data*, to be submitted for publication.
(4) Schwartz, A. S.; Donnelly, H. G. *Chem. Eng. Prog. Symp. Ser.* **1968**, *64*, 44.
(5) Stead, K.; Williams, J. M. *J. Chem. Thermodyn.* **1980**, *12*, 265.
(6) Leu, A.-D.; Robinson, D. B. *J. Chem. Eng. Data* **1988**, *33*, 313.
(7) Pozo, M. E.; Streett, W. B. *J. Chem. Eng. Data* **1983**, *29*, 324.
(8) Chang, E.; Calado, J. C. G.; Streett, W. B. *J. Chem. Eng. Data* **1982**, *27*, 293.
(9) Tsang, C. Y.; Streett, W. B. *J. Chem. Eng. Data* **1981**, *26*, 155.
(10) Soave, G. *Chem. Eng. Sci.* **1972**, *27*, 1197.
(11) Peng, D.; Robinson, D. B. *Ind. Eng. Chem. Fundam.* **1976**, *15*, 59.
(12) Panagiotopoulos, A. Z.; Reid, R. C. In *Equations of State*; Chao, K. C., Robinson, R. L., Eds.; ACS Symposium Series 300; American Chemical Society: Washington, DC, 1986; p 570.

Received for review May 23, 1989. Accepted March 5, 1990. This work was supported by the National Science Foundation under Grant No. CPE-8104708.

Liquid-Phase Excess Enthalpies for the Binary Systems of 1,3-Dioxolane with *n*-Pentane, 3-Methylpentane, or Methylcyclopentane

Fabio Comelli

Centro di Studio per la Fisica delle Macromolecole del CNR, via Selmi 2, 40126 Bologna, Italy

Romolo Francesconi*

Dipartimento di Chimica G. Ciamician, Università degli Studi, via Selmi 2, 40126 Bologna, Italy

Enthalpies of mixing H^E for the binary systems of 1,3-dioxolane with *n*-pentane, 3-methylpentane, or methylcyclopentane were measured by means of an isothermal flow microcalorimeter as a function of composition, under atmospheric pressure and at 298.15 K. All these systems show endothermic mixing with maxima at a mole fraction of about 0.5. Qualitative considerations are added to explain the effects of branching and cyclization on H^E.

Introduction

As a continuation of a long-term study on the thermodynamic properties of mixtures containing 1,3-dioxolane as a common solvent, we report in the present paper the liquid-phase enthalpies of mixing (excess enthalpies) for the binary systems of 1,3-dioxolane with *n*-pentane, 3-methylpentane, or methylcyclopentane.

Other authors have studied the excess enthalpies for mixtures of several cyclic diethers with *n*-alkanes of different chain length (*1*, *2*).

Taking as a basis the pentane structure, the purpose of this paper is also to study the effects of ring closure, the increasing number of ring atoms and side groups in the cyclic structure on the energy interactions responsible for the measured excess enthalpies when mixtures with 1,3-dioxolane are considered.

Chemicals

1,3-Dioxolane, Fluka product, purum, analytical grade 99%, was allowed to stand over a saturated solution of sodium bisulfite so as to remove any aldehydes. It was further purified by refluxing for about 10 h over Na wire in N flow, then distilled over Na, and finally fractionated on a Vigreux column. The fraction boiling in the range 347–348 K was collected.

Methylpentane and methylcyclopentane were Carlo Erba products, analytical grade respectively 99% and 98.5%, while *n*-pentane was a Merck product, analytical grade 99%.

The commercial products were purified by passing through a column filled with silver nitrate on alumina, to remove traces of olefins and aromatics, and then fractionated.

The pure liquids were finally stored over molecular sieves type 4A (C. Erba). After these treatments, a gas chromatographic analysis gave no evidence of significant impurities.

Table I. Densities ρ of Pure Components as a Function of Temperature T; Coefficients A and B, Equation 1; Standard Deviations $\sigma(\rho)$,; and Correlation Coefficients R

	n-pentane		3-methylpentane		methylcyclopentane	
	T/K	ρ/(kg m^{-3})	T/K	ρ/(kg m^{-3})	T/K	ρ/(kg m^{-3})
	295.75	623.96	293.35	664.25	293.55	748.30[c]
	296.25	623.53	294.15	663.50	295.55	746.51
	297.05	622.77	294.85	662.81	296.75	745.37
	298.65	621.14[a]	296.15	661.75	299.35	742.89
	299.35	620.41	297.25	660.66	299.85	742.40
	300.75	619.10	298.25	659.94[b]	303.15	739.28
	301.65	618.12	298.75	659.33	303.75	738.69
			299.45	658.67	304.75	737.94
			302.25	656.14	305.95	736.68
			303.45	654.95	306.45	736.14
A	646.372		682.753		767.571	
B	−0.989 96		−0.916 06		−0.943 01	
$\sigma(\rho)$	0.03		0.06		0.02	

R = 0.999

[a] At T = 298.15; ρ = 621.39 (9). [b] At T = 298.15; ρ = 659.76 (8). [c] At T = 293.15; ρ = 748.64 (8).

Calorimetric Measurements

Calorimetric measurements at 298.15 K were made by means of an LKB Model 2107 flow microcalorimeter (LKB, Produkter AB, Bromma, Sweden) described elsewhere (*3*). Details on calibration, analytical measurements, and the accuracy of the results are given in ref 4. The performance of the

0021-9568/90/1735-0283$02.50/0